

Magnetic circular dichroism of $3d_{5/2} \rightarrow 2p_{3/2}$ resonant inelastic X-ray scattering at the Ho L_{III} -edge in $\text{Ho}_3\text{Fe}_5\text{O}_{12}$

Tetsuya Nakamura,^{a*} Naomi Kawamura,^b Toshiaki Iwazumi,^c Hiroshi Maruyama,^d Akiri Urata,^d Hironobu Shoji,^e Susumu Nanao,^e Shunji Kishimoto,^c Rintaro Katano^f and Yasuhito Iozumi^g

^aRIKEN, 2-1 Hirosawa, Wako, Saitama 351-0198 Japan, ^bRIKEN/SPRING-8, 1-1-1 Kouto, Mikaduki, Hyogo 679-5148 Japan, ^cPhoton Factory, Institute of Materials Structure Science, 1-1 Oho, Tsukuba 305-0801 Japan, ^dDepartment of Physics, Faculty of Science, Okayama University, 3-1-1 Tsushima-Naka, Okayama 700-8530 Japan, ^eInstitute of Industrial Science, University of Tokyo, Tokyo 106-8558, Japan, ^fInstitute for Chemical Research, Kyoto University, Uji 611-0011 Japan, and ^gRadioisotope Research Center, Kyoto University, Kyoto 606-8501 Japan. E-mail: naka@postman.riken.go.jp, FAX: +81-48-462-4649

Magnetic Circular Dichroism (MCD) of Resonant Inelastic X-ray Scattering (RIXS) of $3d_{5/2} \rightarrow 2p_{3/2}$ decay (Ho $L\alpha_1$) was measured at the Ho L_{III} -edge in $\text{Ho}_3\text{Fe}_5\text{O}_{12}$. The MCD-RIXS, in which the intermediate state has the $2p4f^{n+1}$ configuration due to the quadrupolar transition of $2p \rightarrow 4f$, was also observed at the pre-edge region of the Ho L_{III} -edge. The obvious superposition of two peaks, which comes from the high-energy off-resonant Raman scattering and the fluorescence, could be found in both the RIXS and the MCD-RIXS when the energy of the incoming X-ray was 7 eV higher than the white line. The dependence of the integration of the MCD-RIXS spectra on the incident x-ray energy could roughly reproduce the MCD of X-ray absorption spectra (XAS).

Keywords: magnetic circular dichroism; resonant inelastic x-ray scattering; $\text{Ho}_3\text{Fe}_5\text{O}_{12}$.

1. Introduction

Resonant Inelastic X-ray Scattering (RIXS) has become a powerful tool to investigate the electronic structures in solid-state materials thanks to intense and tunable X-rays at synchrotron facilities. The spin-dependent part of RIXS could be observed as the Magnetic Circular Dichroism (MCD) and provides knowledge of the precise spin dependence of the electronic structure. The origin of the MCD effect of an off-resonant x-ray emission is well understood up to now. In the case of rare earth ions, theoretical calculations of the lineshapes (de Groot *et al.*, 1997; Jo *et al.*, 1998) were possible for the decays of $3d \rightarrow 2p$ and $4d \rightarrow 2p$, and have been also confirmed experimentally (Iwazumi *et al.*, 2000). The dependence of MCD-RIXS on the incident x-ray energy (Ω) around the absorption edge has been, however, reported only for Gd ions in Gd metal by Krisch *et al.* (1996) and in ferrimagnetic $\text{Gd}_{33}\text{Co}_{67}$ amorphous alloy by the present authors (Iwazumi *et al.*, 1997). MCD-RIXS could help to interpret the conventional MCD of X-ray absorption because RIXS is the second-order optical process, where the intermediate state of RIXS coincided with the final state of XAS.

MCD-RIXS seemed to be especially effective to elucidate the origin of MCD-XAS at the pre-edge region in which a quadrupolar transition to the $4f$ state was thought to exist. In this study, MCD-RIXS of a ferromagnetic Ho ion in ferrimagnetic $\text{Ho}_3\text{Fe}_5\text{O}_{12}$ was measured for the $3d_{5/2} \rightarrow 2p_{3/2}$ decay at the Ho L_{III} -edge. The dependence of the spectral features of MCD-RIXS is discussed comparing with the MCD-XAS at the Ho L_{III} -edge, which has been reported by Shimomi *et al.* (1993).

2. Experimental

A single crystal of ferrimagnetic $\text{Ho}_3\text{Fe}_5\text{O}_{12}$ was studied at room temperature, where the magnetic moment of Ho ions couples antiparallel with respect to the total magnetization. The MCD-RIXS experiments were performed at the elliptical multi-pole wiggler beamline 28B (Iwazumi *et al.*, 1995) of the Photon Factory, Institute of Materials Structure Science. The degree of circular polarization, P_c , of the incident X-rays monochromatized using Si(220) reflection is about -0.45 of a minus helicity at the Ho L_{III} -edge. The geometrical layout of the present experiment around a sample is shown in Figure 1, where the angle between the scattered X-rays and the normal of sample surface was set to 54.7 degrees, the so-called magic angle (de Groot *et al.*, 1997). The angle between incident X-rays and the sample magnetization (θ) was chosen to be 36.9 degrees to get the best compromise between the energy resolution of the emission spectra and the magnitude of the MCD signals, which is proportional to $\cos \theta$. A magnetic field of 0.2 T was applied to the sample, and its direction switched every 10 seconds to obtain the MCD effect without changing the helicity of the incident x-rays. The emitted X-rays were analyzed using a cylindrical bent Ge(440) crystal and a position-sensitive proportional counter filled with an Ar + 10% CH_4 mixture of 8 atm. The total energy resolution of the present apparatus was 1.6 eV around the Ho $L\alpha_1$ fluorescence line (6718 eV). RIXS and MCD-RIXS were defined by eq. (1) and (2) respectively, as follows:

$$I_0(\omega) = \{I_+(\omega) + I_-(\omega)\}/2, \quad (1)$$

$$I_m(\omega) = I_+(\omega) - I_-(\omega). \quad (2)$$

Here, $I_+(\omega)$ and $I_-(\omega)$ are the intensities of the fluorescence yield and were measured with the wave vector (\mathbf{k}) of the incident beam parallel and anti-parallel to the magnetization of a sample, respectively, where ω denotes the energy of emitted X-rays. The intensity of incoming X-rays was monitored using ion chamber and was used as normalization factor of $I_+(\omega)$ and $I_-(\omega)$.

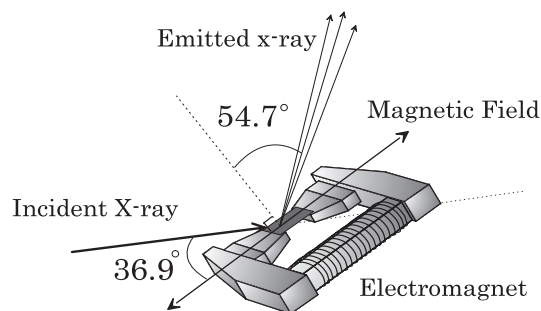


Figure 1

Schematic diagram of the experimental layout around a sample for measurements of MCD-RIXS. The electromagnet produces magnetic field of 0.2 T at the beam-spot on the sample.

3. Results and Discussion

The MCD of the X-ray Absorption Spectrum (XAS) at the Ho L_{III} -edge in $\text{Ho}_3\text{Fe}_5\text{O}_{12}$ was quoted from the previous report by Shimomi *et al.*, (1993) and is reproduced in Figure 2.

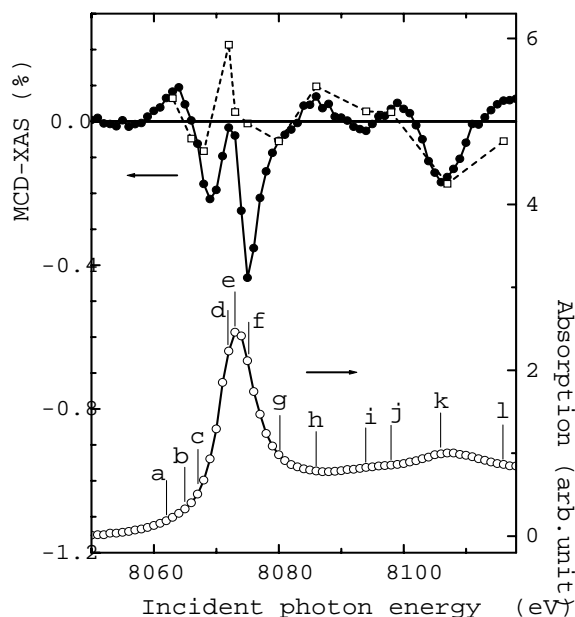


Figure 2

Reproduced XAS (open circle) and MCD-XAS (filled circle) at the Ho L_{III} -edge in a $\text{Ho}_3\text{Fe}_5\text{O}_{12}$ at room temperature (Shimomi *et al.*, 1993). The vertical lines with labels from *a* to *l* on XAS correspond to the energies at which MCD-RIXS were measured. The values of $S_m(\Omega)$ (open square) are also plotted using an arbitrary scale.

MCD-RIXS spectra were measured at the energies which are indicated by vertical lines labelled *a* ~ *l* in Fig. 2. Figure 3 shows the RIXS and the MCD-RIXS for $3d_{5/2} \rightarrow 2p_{3/2}$ decays in the Ho ion, where the labels from *a* to *l* are consistent with those in Fig. 2. The Ω -dependence of the peak height of the emission line in RIXS looked very similar to XAS (not shown here). In addition to the Raman shifts below the energy *d*, the off-resonant Raman peaks to the high-energy region were also observed in the RIXS spectra from *g* to *i*. The linear fitting of the positions of Raman peaks from *a* to *d* gave the relation between Ω and ω as $\omega = 1.02 \times \Omega - 1499.6\text{eV}$. The asymmetric shape at the low energy side of the emission line originates multiplet effect mainly due to the $3d$ - $4f$ exchange interaction. Despite the single peak feature of emission line at *f*, there was small overshoots of the peak shift due to the superposition between the high-energy off-resonant contribution and the fluorescence line ($L\alpha_1$), where the fluorescence and the off-resonant Raman scattering correspond to the transition into the continuum state and the transition into the $5d$ state, respectively. The maximum amplitude of the MCD-RIXS is found at *f*, which is about +1.7 % of the peak height of the RIXS. The amplitude itself does not change so much depending on Ω despite the complicated structure of MCD-XAS. Taking into account the statistical accuracy of MCD-RIXS spectra in Fig. 3, the overall spectral features of the MCD-RIXS from *a* to *l* were similar to each other except for those at *a* and *g*. It has been suggested that the pre-edge feature in MCD-XAS at the energy *a* arises from a quadrupolar transition to the $4f$ state, based on the assumption that the interaction between the

$2p$ core hole and the $4f$ electrons lowers the $4f$ level energy below the pre-edge region. The theoretical angular dependence of the quadrupolar contribution in MCD-XAS has not been confirmed in this system because the difference between the quadrupolar and the dipolar contribution might be too small to be detected at room temperature due to thermal fluctuations. In the MCD-RIXS spectra at *a* and *b*, the MCD-RIXS coming from the quadrupolar channel was observed with a satisfactory separation of 10.8 eV from the dipolar channel. The MCD-RIXS spectrum at *g* looked rather different from the others due to the superposition of the two different MCD that originated from the fluorescence and the high-energy off-resonant Raman scattering.

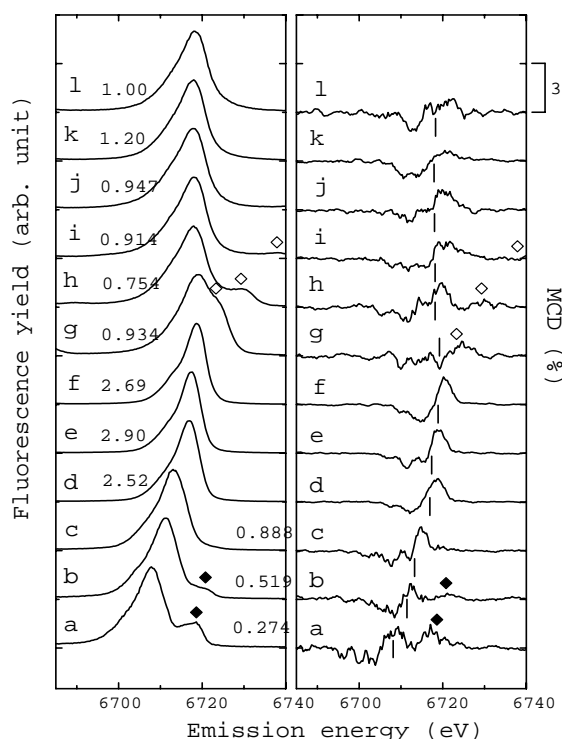


Figure 3

RIXS (left panel) and MCD-RIXS (right panel) of $3d_{5/2} \rightarrow 2p_{3/2}$ decay at the Ho L_{III} -edge in $\text{Ho}_3\text{Fe}_5\text{O}_{12}$. The labels from *a* to *l* indicate the energies of incident X-rays and are consistent with those used in Fig. 2. The series of numbers in the left panel are the relative intensities of RIXS spectra. The vertical lines in the right panel correspond to the energies of peaks in RIXS spectra. The filled and the open diamonds are marked at the positions of RIXS peaks of the quadrupolar channel and the high-energy off-resonant Raman peak in the both panels, respectively.

The integration of MCD-RIXS changed depending on Ω and could be possible to compare them with the intensity of MCD-XAS at the Ω . Then, $S_m(\Omega)$, which was defined as $S_m(\Omega) = \int I_m(\omega)d\omega$, was calculated to discuss the integrations from 6685 eV to 6740 eV. The result shown in Fig. 2 indicates that the tendency of the Ω dependence of the $S_m(\Omega)$ roughly agrees with the spectral feature of the MCD-XAS. Because of the existence of the positive peak originated from the quadrupolar channel at *a*, the sign of integration of MCD-RIXS spectrum was the positive and coincided with the sign of MCD-XAS. The large disagreements are found at the energy region of *d* ~ *f* locating near the white-line. The

disagreements seem to come from the differences of the present experimental conditions between MCD-XES in Fig.3 and MCD-XAS in Fig. 2, such as magnetic fields applied to a sample and the angle θ . It might be also necessary to consider contributions from other emissions such as $L\beta_{2,15}$ lines in spite that MCD-RIXS for the $3d_{5/2} \rightarrow 2p_{3/2}$ emission was much more dominant than them.

4. Summary

The Ω -dependence of MCD-RIXS of the $3d_{5/2} \rightarrow 2p_{3/2}$ decay was demonstrated at the Ho L_{III} -edge in $\text{Ho}_3\text{Fe}_5\text{O}_{12}$. The RIXS peak and the MCD-RIXS of the quadrupolar channel were observed at the pre-edge region of the Ho L_{III} -edge, where the energy separation between the quadrupolar and the dipolar was determined to be +10.8 eV in the RIXS spectra. The MCD of the fluorescence was superimposed strongly on that of the high-energy off-resonant Raman scattering at g , when the energy of the incoming X-ray was 7eV higher than the white line. The Ω dependence of the integrations of MCD-RIXS almost coincided with the MCD-XAS except for that just on the white-line.

The authors would like to thank Prof. A. Kotani, Prof. I. Harada, Dr. H. Ogasawara, and Dr. K. Fukui for useful discussions about

emission spectroscopy. This work has been performed with the approval of the Photon Factory Program Advisory Committee (Proposal No. 97G279 and 97G287). One of the present authors (T. N.) is supported by RIKEN and was partially supported by Grant-in-Aid for Scientific Research from the Japanese Ministry of Education, Science, Sports and Culture.

References

- de Groot, F. M. F., Nakazawa, M., Kotani, A., Krisch, M. H. & Sette, F. (1997). *Phys. Rev. B* **56**(12), 7285–7292.
- Iwazumi, T., Kobayashi, K., Kishimoto, S., Nakamura, T., Nanao, S., Oh-sawa, D., Katano, R. & Isozumi, Y. (1997). *Phys. Rev. B* **56**(22), R14 267-R14 270.
- Iwazumi, T., Nakamura, T., Shoji, H., Kobayashi, K., Kishimoto, S., Katano, R., Isozumi, Y. & Nanao, S. (2000). *J. Phys. Chem. Sol.* **61**, 453–456.
- Iwazumi, T., Koyama, A. & Sakurai, Y. (1995). *Rev. Sci. Instrum.* **66**, 1691–1693.
- Jo, T. & Tanaka, A. (1998). *J. Phys. Soc. Jpn.* **67**, 1457–1465.
- Krisch, M. H., Sette, F., Bergman, U., Masciovecchio, C., Verbeni, R., Goulon, J., Caliebe, W. & Kao, C. C. (1996). *Phys. Rev. B* **54**(18), R12 673-R12 676.
- Shimomi, K., Maruyama, H., Kobayashi, K., Koizumi, A., Yamazaki, H. Iwazumi, T. (1993). Proc. 7th Int. Conf. XAFS, Kobe, 1992, *Jpn. J. Appl. Phys.* **32**, Suppl. **32-2**, 314–316.